The Effects of High Power Diode Laser Radiation on the Wettability, Adhesion and Bonding Characteristics of an Alumina/Silica-Based Oxide and Vitreous Enamel

J. Lawrence *, L. Li * and J.T. Spencer **

* Manufacturing Division, Department of Mechanical Engineering, University of Manchester Institute of Science and Technology (UMIST), Manchester, M60 1QD, UK.

** Research & Technology, B709, BNFL, Springfields Works, Salwick, Preston, Lancashire, PR4 0XJ, UK.

Correspondence

Mr. Jonathan Lawrence / Dr. Lin Li

Manufacturing Division,

Department of Mechanical Engineering,

University of Manchester Institute of Science and Technology (UMIST),

Manchester,

M60-1QD,

UK.

Tel : (44) 161 236-3311 ext. 2383 / (44) 161 236-3311 ext. 3816

Fax : (44) 161 200-3803

e-mail : j.lawrence@stud.umist.ac.uk / L.Li@umist.ac.uk

ABSTRACT

An amalgamated alumina/silica-based oxide compound (AOC) was surface treated using a 60 W high power diode laser (HPDL). The effects of HPDL radiation on the wettability and adhesion characteristics of the AOC and a vitreous enamel have been determined. The basic process phenomena are investigated and the effects of laser irradiation in terms of composition and microstructure are presented. Without laser treatment of the AOC surface it was not possible to fire the enamel onto the AOC. However, wetting experiments using a number of control liquids, by the sessile drop technique, revealed that laser treatment of the AOC surface resulted in the polar component of the surface energy increasing after laser treatment from 2.00 mJm^{-2} to 16.15 mJm^{-2}. Additionally, surface roughness measurements revealed that after laser treatment, the surface roughness had decreased from an Ra value of 25.85μm to 6.27μm, whilst an energy disperse X-ray analysis (EDX) revealed that the relative surface oxygen content of the AOC had increased by 36.29% after laser treatment. Thus, laser treatment was identified as effecting a decrease in the enamel contact angle from 118^{0} to 33^{0}; consequently allowing the vitreous enamel to wet the surface. The bonding mechanisms were identified as being principally due to van der Waals forces, however, some evidence of chemical bonding was observed. The work has shown clearly that laser radiation can be used to alter the wetting characteristics of the AOC.

Keywords: high power diode laser, surface energy, wettability

1. Introduction

The understanding of the interfacial phenomena between vitreous enamels and ceramic materials is of great interest in both engineering and scientific fields. In many technological applications where vitreous enamels are fired onto ceramic substrates, the performance of the article is directly linked to the nature of the enamel-ceramic interface. Many studies to investigate these phenomena have been carried out, however, they have been principally concerned with the wettability of zirconia and other oxide ceramics on metals [1-5] as well as the adhesion of silicone sealants to aluminium [6] and the coating of aluminium alloys with ceramic materials [7, 8]. The interfacial mechanisms investigated have centred principally around the thermodynamic criterion [2, 3, 5], the electronic theory [4] and the occurrence of oxidation [1, 9].

To date, very little work has been published with regard to the use of lasers for modifying surface properties of materials in order to improve their wettability characteristics. Notwithstanding this, it is recognised within the currently published work that laser irradiation of material surfaces can effect its wettability characteristics. Previously Zhou et al [7, 8] have carried out work on laser coating of aluminium alloys with ceramic materials (SiO_2, Al_2O_3, etc), reporting on the well documented fact that generated oxide layers often promote metal/oxide wetting. Bahners et al [10, 11], have observed and comprehensively detailed the changes in technical properties of various textile fibres, including adhesion and wetting properties, with a view to developing an alternative to the conventional methods of chemical agents addition or wet-chemical pre-processing. However, the reasons for these changes with regard to changes in the material's surface tension are not reported.

The technique described in this paper, that of using high power diode laser (HPDL) beams to determine the effects of laser radiation on the wettability characteristics and bonding mechanisms of an amalgamated alumina/silica-based oxide compound (AOC) mix and a vitreous enamel, has been employed by the authors to enable the sealing, by means of laser enamelling, of ceramic tile grouts [12].

2. Theoretical background

2.1 Contact angle and wettability

When a drop of liquid is placed on a solid surface it may remain as a spherical drop, or spread to cover (wet) the solid surface [13]. The angle with which the liquid subtends the solid is known as the contact angle. In practice, for wetting to occur the contact angle is less than 90^0. If the contact angle is greater than 90^0 then the liquid does not wet the solid and no adhesion occurs [13]. Once irradiated by the HPDL beam the enamel powder melts, transforming to a liquid phase. As such, the process of the bonding of the enamel to the AOC substrate is determined by the wettability of the two component parts. When a drop of liquid is brought into contact with a flat solid surface, the final shape taken by the drop, and thus whether it will wet the surface or not, depends upon the relative magnitudes of the molecular forces that exist within the liquid (cohesive) and between the liquid and the solid (adhesive) [13]. The index of this effect is the contact angle θ, which the liquid subtends with the solid. θ is related to the solid and liquid surface energies, γ_{sv} and γ_{lv}, and the solid-liquid interfacial energy γ_{sl}, through the principle of virtual work expressed by the rearranged Young's equation:

$$\cos\theta = \frac{\gamma_{sv} - \gamma_{sl}}{\gamma_{lv}} \tag{1}$$

Clearly, to achieve wetting γ_{sv} should be large, while γ_{sl} and γ_{lv} should be small. Hence liquids of a lower surface tension will always spread over a solid surface of higher surface tension in order to reduce the total free-energy of the system [14]. This is due to fact that the molecular adhesion between solid and liquid is greater than the cohesion between the molecules of the liquid [13].

The adhesion energy of a liquid to a solid surface (the work of adhesion) W_{ad}, is given by the Young-Dupre equation:

$$W_{ad} = \gamma_{lv}\left(1 + \cos\theta\right) \tag{2}$$

4

It is important to consider also the influence of the substrate surface roughness on the wetting contact angle. According to Neumann [15], a model similar to that for heterogeneous solid surfaces can be developed in order to account for surface irregularities, being given by Wenzel's equation:

$$r\left(\gamma_{sv} - \gamma_{sl}\right) = \gamma_{lv}\cos\theta_w \tag{3}$$

where,   r = Roughness factor defined as the ratio of the real and apparent surface areas

θ_w = Contact angle for the wetting of a rough surface

Clearly, as Equation (3) shows, the influence of surface roughness on the contact angle is to affect an increase in the contact angle. Thus, the smoother the contact surface is, then the smaller the contact angle will be.

2.2 Surface energy and the polar/dispersive characteristics

The intermolecular attraction which is responsible for surface energy, γ, results from a variety of intermolecular forces whose contribution to the total surface energy is additive [16]. The majority of these forces are functions of the particular chemical nature of a certain material, and as such the total surface energy comprises of γ^p (polar or non-dispersive interaction) and γ^d (dispersive component; since van der Waals forces are present in all systems regardless of their chemical nature). Therefore, the surface energy of any system can be described by [16]

$$\gamma = \gamma^d + \gamma^p \tag{4}$$

Similarly, W_{ad} can be expressed as the sum of the different intermolecular forces that act at the interface [16]:

$$W_{ad} = W_{ad}^d + W_{ad}^p = 2\left(\gamma_{sv}^d \gamma_{lv}^d\right)^{1/2} + 2\left(\gamma_{sv}^p \gamma_{lv}^p\right)^{1/2} \tag{5}$$

By equating Equation (5) with Equation (2), the contact angle for solid-liquid systems can be related to the surface energies of the respective liquid and solid by

$$\cos\theta = \frac{2\left(\gamma_{sv}^{d}\gamma_{lv}^{d}\right)^{1/2} + 2\left(\gamma_{sv}^{p}\gamma_{lv}^{p}\right)^{1/2}}{\gamma_{lv}} - 1 \qquad (6)$$

3. Experimental procedures

3.1 Materials

A newly developed ceramic tile grout compound consisting of mixed vitrifiable oxide powders such as chamotte (mainly SiO_2 (53wt%) and Al_2O_3 (42wt%)), Fe_2O_3, MgO, ZrO_2 and ZnO was produced. The oxide powders were sieved to ensure a particle size of less than 75μm, then thoroughly mixed together to ensure homogeneity, along with approximately 50wt% diluted sodium silicate solution so as to form a manageable paste. The AOC was then pasted on to an ordinary Portland cement (OPC) substrate to a thickness of 2mm and allowed to cure at room temperature for 12 hours. The set compound was then irradiated using the HPDL and immediately pasted over with a thin layer (250μm) of commercially available enamel frit (Ferro Ltd.) which, in order to form a manageable paste, was mixed with 20wt% white spirit. The composition of the enamel consisted mainly of the following; SiO_2, B_2O_3, Na_2O, Mn, F and small quantities of Ba, Al_2O_3 and Ni, whilst the powder size was less than 75μm. The enamel frit paste was allowed to cure at room temperature for one to two hours and then irradiated immediately with the HPDL beam.

3.2 Laser processing procedure

The laser used in the study was a surgical HPDL (Diomed Ltd.), emitting at 810nm ±20nm and operating in the CW mode with rated optical powers ranging from 0-60 W. The laser beam was delivered to the work area by means of a 4m long, 600μm core diameter optical fibre, the end of which was connected to a 2:1 focusing lens assembly mounted on the z-axis of a 3-axis CNC gantry table. The AOC was irradiated using the defocused high order mode HPDL beam with a beam spot diameter of 1.75mm and laser powers (measured at the workpiece using a Power Wizard power meter) of 20-55 W. Fig. 1 illustrates the laser processing experimental arrangement, where the

defocused laser beam was fired across the surface of the AOC by traversing the samples beneath the laser beam using the x- and y-axis of the CNC gantry table at speeds ranging from 5-8 mms^{-1}, whilst 3 lmin^{-1} of coaxially blown O_2 assist gas was used to shield the laser optics.

In order to analyse the laser treated specimens, they were sectioned with a Struers cutting machine using a diamond rimmed cutting blade, and then polished using cloths and diamond suspension pastes down to 3μm. The sectioned samples were then examined using optical microscopy, scanning electron microscopy (SEM), energy disperse X-ray analysis (EDX) and X-ray diffraction (XRD) techniques.

3.3 Wetting and surface energy analysis procedures

To examine the wetting and surface energy characteristics of the AOC two sets of wetting experiments were conducted. The first set of experiments were to simply determine the contact angle between the enamel and the AOC before and after laser treatment. The second set of experiments were control experiments carried out using a variety of liquids with known surface energy properties in order to quantify any surface energy changes in the AOC resulting from laser irradiation.

The enamel-AOC wetting experiments were carried out in atmospheric conditions with molten droplets of the enamel (600^{0}C). The temperature of the enamel throughout the experiments was measured using a Cyclops infrared pyrometer. The droplets were released in a controlled manner onto the surface of the AOC (treated and untreated) from the tip of a micropipette, with the resultant volume of the drops being approximately 15 x 10^{-3} cm^3. Profile photographs of the sessile enamel drop were obtained for every 60^{0}C fall in temperature of the molten enamel drop, with the contact angle subsequently being measured.

The control experiments were carried out using: human blood, human blood plasma, glycerol and 4-octanol. The test liquids, along with their total surface energy (γ_2) as well as the dispersive (γ_{lv}^d) and polar (γ_{lv}^p) components, are detailed in Table I. The experiments were conducted in atmospheric conditions at a temperature of 20^{0}C with the temperature of the liquids themselves throughout the experiments also being maintained at 20^{0}C. The droplets were released in a controlled manner onto the surface of the test substrate materials (treated and untreated) from the tip of a micropipette, with the resultant volume of the drops being approximately 6 x 10^{-3} cm^3. Each experiment lasted for three

minutes with profile photographs of the sessile drops being obtained every minute, with the contact angle subsequently being measured.

4. Effects of laser radiation on the amalgamated oxide compound

In order to bond together the oxide compounds the amalgamation was mixed with 50wt% diluted sodium silicate solution. Sodium silicate solution (waterglass) is a viscous colourless solution of colloidal sodium silicate. It is a silica containing aqueous solution that, when combined with other solutions such as the amalgamated oxide compound, forms a gel-like mass of silicate hydrate. Such a mass remains soft and malleable until it is exposed to CO_2 gas, either by means of a gas jet or through contact with the atmosphere [17]. But, exposure of the hardened mass to water results in a reversing of the process and the mass returns to a gel-like state.

The fact that the AOC in an un-heated state is hydraulically bonded, as opposed to chemically bonded, combined with the retention of chemical and mechanical water (that is water that is bonded into the materials matrix and additional free-water respectively) means that the hardened mass will rehydrate when exposed to water [17, 18]. Heating of the hardened AOC mass fires the waterglass (similar to that of a ceramic material) [17], increasing its strength and enabling it to withstand water exposure. Thus, heating of the AOC is similar in effect to the firing of ceramics, in that the heating causes gradual ceramic 'sintering' of the materials; generally bonding together and stabilising the substances [17, 19]. As such, exposure of the AOC to laser radiation results in rapid heating of the surface, for most materials typically 10^3-10^5 $^0Cs^{-1}$ [20], which will lead to such sintering of the AOC surface with the removal of the pores between the starting particles of the compound, combined with growth together and strong bonding between adjacent particles [21], thus, a much more consolidated surface is created. Indeed, surface roughness measurements revealed that the surface roughness had decreased from an Ra value of 25.85μm before laser treatment, to 6.27μm after laser treatment. Also, it was found that heating of the AOC above 100^0C resulted in sufficient pyrochemical changes to prevent any rehydration.

From Fig. 2(a) it can be seen clearly that before laser treatment the surface of the AOC appears coarse, with individual crystals of the constituent components being clearly discernible. After laser treatment (Fig. 2(b)) there is more surface ordering, with the surface appearing cellular-dendritic,

showing that fusion of the individual particulates has occurred. Such a solidification structure is indicative of rapidly solidified microstructures [22]. Moreover, an XRD analysis of the AOC surface before and after laser treatment (Fig. 3) revealed that, on the whole, the phases present within the laser treated region were the same, however, their proportions were different. In particular, after laser treatment it was not possible to detect any SiO_2 whilst the Al_2O_3 was depleted. But, as the EDX analysis shows (Fig. 4) Si and Al were still present in similar proportions on the AOC surface before and after laser treatment. This indicates that partial laser vitrification of the AOC surface has occurred due to the fact that these materials are glass forming elements, and as such, vitrified when irradiated.

5. Wettability and surface energy characteristics

5.1 Contact angle and wettability

An optical micrograph of a sessile drop of enamel (20^0C) placed on the surface of the AOC before (a) and after (b) laser irradiation with the contact angle superimposed is shown in Fig. 5. The experimental results showed that throughout the period of cooling of the enamel, from the molten state at 600^0C to the solid state at room temperature, no discernible change in the magnitude of the of the contact angle took place during the time of the experiments. This indicates that thermodynamic equilibrium was established at the solid-liquid interface at the outset of the experiment [23].

Fig. 5 shows clearly that prior to laser treatment it was not possible to fire the enamel onto the surface of the AOC since the contact angle was measured as 118^0, and as such would prevent the enamel from wetting the AOC surface. Indeed, laser interaction with the enamel when placed on the untreated AOC surface simply resulted in the 'balling' of the enamel; the formation of small spheres approximately the diameter of the laser beam itself [24, 25]. One explanation for the fact that laser treatment of the AOC is necessary so that the enamel completely wets and adheres to the surface of the AOC is that the surface resulting from the laser treatment is significantly smoother, with an Ra value of 25.85μm compared with 6.27μm, and, according to Equation (3), will intrinsically affect a reduction in the contact angle. Also, wetting will have certainly been influenced by the increase in the oxygen content of the AOC surface as a result of the laser treatment, since this is known to increase the likelihood of wetting [1, 9]. Indeed, by mounting cross-sectioned samples of the untreated and

laser treated AOC next to each other, and examining them both simultaneously by means of EDX, it is possible to determine the relative element content of oxygen near to the surface. Values of 28.27% and 38.53% for the untreated and laser treated AOC respectively were obtained from such an EDX analysis which probed to a depth of approximately 1μm below the surface of both samples. As one can see, an increase of 36.29% in the amount of oxygen due to the oxidisation on the laser treated surface of AOC has occurred, indicating that oxygen enrichment of the laser treated AOC surface is active in promoting wetting and bonding.

5.2 Amalgamated oxide compound surface energy and its dispersive/polar character

It is possible to adequately estimate the dispersive component of the AOC surface energy γ_{sv}^{d} by using Equation (6), and plotting the graph of cos θ against $(\gamma_{lv}^{d})^{1/2}/\gamma_{lv}$. Thus the value of γ_{sv}^{d} is estimated by the gradient $(=2(\gamma_{sv}^{d})^{1/2})$ of the line which connects the origin (cos θ = -1) with the intercept point of the straight line (cos θ against $(\gamma_{lv}^{d})^{1/2}/\gamma_{lv}$) correlating the data point with the abscissa at cos θ = 1 [16]. Fig. 6 shows the best-fit plot of cos θ against $(\gamma_{lv}^{d})^{1/2}/\gamma_{lv}$ according to Equation (6) for the untreated and laser treated AOC-experimental control liquids system. Comparing the ordinate intercept points of the untreated and laser treated AOC-liquid systems, it can be seen clearly from Fig. 6 that for the untreated AOC-liquid systems the best-fit straight line intercepts the ordinate closer to the origin. This indicates that, in principle, dispersion forces act mainly at the AOC-liquid interfaces resulting in poor adhesion [16, 26]. In contrast, Fig. 6 shows that the best-fit straight line for the laser treated AOC-liquid systems intercepts the ordinate considerably higher above the origin. This is indicative of the action of polar forces across the interface, in addition to dispersion forces, hence improved wettability and adhesion is promoted [16, 26].

It is not possible to determine the value of the polar component of the AOC surface energy γ_{sv}^{p} directly from Fig. 6. This is because the intercept of the straight line (cos θ against $(\gamma_{lv}^{d})^{1/2}/\gamma_{lv}$) is at $2(\gamma_{sv}^{p}\gamma_{lv}^{p})^{1/2}/\gamma_{lv}$, and thus only refers to individual control liquids and not the control liquid system. However, it has been established that the entire amount of the surface energies due to dispersion forces either of the solids or the liquids are active in the wettability performance [16, 27]. Thus it is

possible to calculate the dispersive component of the work of adhesion, W_{ad}^d from Equation (5). The results reveal that for each particular control liquid in contact with both the untreated and laser treated AOC surfaces, W_{ad} can be correlated with W_{ad}^d by the relationship

$$W_{ad} = aW_{ad}^d + b \qquad (7)$$

Also, for the control test liquids used, a linear relationship between the dispersive and polar components of the control test liquids surface energies has been deduced which satisfies the equation

$$\left(\gamma_{lv}^p\right)^{1/2} = 1.3\left(\gamma_{lv}^d\right)^{1/2} + 1.15 \qquad (8)$$

By introducing Equation (7) into Equation (5) and rearranging, then

$$W_{ad}^p = (a-1)W_{ad}^d + b \qquad (9)$$

By combining Equation (9) with Equation (5) and differentiating with respect to $\left(\gamma_{lv}^d\right)^{1/2}$, then the following can be derived:

$$\left(\gamma_{sv}^p\right)^{1/2} = \frac{\left(\gamma_{sv}^d\right)^{1/2}(a-1)}{1.3} \qquad (10)$$

From a plot of Equation (9), a can be determined for the untreated and laser treated AOC (1.2 and 1.7 respectively). Since γ_{sv}^d has already been determined for the untreated and laser treated AOC from Fig. 6, then it is possible to calculate γ_{sv}^p for untreated and laser treated AOC using Equation (10).

Table II details the values determined for γ_{sv}^d and γ_{sv}^p for both the untreated and laser treated AOC. Clearly the HPDL treatment of the surface of the AOC leads to a reduction in the total surface energy γ_{sv}, whilst increasing the polar component of the surface energy γ_{sv}^p, thus improving the action of wetting and adhesion. Such changes in the surface energy of the AOC after laser treatment are due to the fact that HPDL treatment of the surface of the AOC results in partial vitrification of the surface; a transition that is known to affect a reduction in γ_{sv} and an increase in γ_{sv}^p [23].

6. Bonding mechanisms

Based on the nature of the attractive forces existing across the liquid-solid interface, wetting can be classified into the two broad categories of physical wetting and chemical wetting. In physical wetting the attractive energy required to wet a surface is provided by the reversible physical forces (van der Waals). In chemical wetting adhesion is achieved as a result of reactions occurring between the mating surfaces, giving rise to chemical bonds [28]. In either case, the driving force for wetting is the reduction of the surface free energy of the solid AOC by the liquid enamel (γ_{sv} - γ_{sl}). Spreading requires the additional contribution to the driving force of the free energy of the interfacial reaction [29].

In practice, complex combinations of various bonding mechanisms actually occur, varying according to the types of materials used [28]. For the AOC and the enamel, the mechanisms involved in ceramic-glass bonding are reasonably applicable. These principally include physical bonding (van der Waals forces), chemical bonding (oxide transformation and O_2 bridging) and on a very small scale, electrochemical reactions such as the electrolytic effect due to the presence of ferric oxides within the AOC reacting with other oxides in the enamel [28]. In the particular case of the AOC and the enamel, the bonding mechanism is principally the result of physical forces. This is because adhesion between many materials is assured by electron transfer and is therefore related to bandgap energy [4, 9]. Thus, for non-conducting materials, such as the AOC, with large bandgaps, there will be practically no free charges inside the ceramic crystals, even at elevated temperatures. In this case the electron transfer at the interface will not take place since the electron transfer depends exclusively on the concentration of free charges in the ceramic crystal [4]. As a result, the chemical contribution to the work of adhesion is negligible since W_{ad} can be expressed as the sum of the different contributions of the interfacial interactions between the two phases [5]:

$$W_{ad} = W_{non-equil} + W_{chem-equil} + W_{vdw} \qquad (11)$$

$W_{non-equil}$ represents the non-equilibrium contribution to the work of adhesion when a chemical reaction takes place at the interface. $W_{chem-equil}$ is the cohesive energy between the two contacting phases, which is resulted from the establishment of the chemical equilibrium bonds achieved by the mutual saturation of the free valences of the contacting surfaces. W_{vdw} is the energy of the van der

Waals interaction. Consequently, the work of adhesion W_{ad}, is chiefly only resulted from the van der Waals interaction.

The bonding mechanism between the laser treated AOC and the enamel, however, was found to be not entirely due to physical forces. An EDX analysis conducted at the interface between the AOC and the enamel revealed the presence of a small diffusion region which contained elements unique to the AOC (Mg, Zr, etc.) and the enamel (Mn, Ni, etc.). This is perhaps to be expected since enamel glazes on ceramic materials, such as the AOC, are typically bonded as a result of some of the base material dissolving into the glaze [28], with wetting characteristics often being achieved or enhanced by a reaction at the interface at an elevated temperature [29]. Also, when the samples were pulled apart in this region, debris from both components was found on each of the two pieces, indicating the possible action of some form of chemical bonding. However, such evidence could also be seen as indicating that the van der Waals bond between the enamel and the AOC was stronger than the actual cohesive forces within the AOC.

As one can see from Fig. 7, there is no dendritic growth in the bond region which is characteristic of enamels fired onto substrates containing Fe, Si and in particular Co [29]. However, it can be seen that enamel is held firm in the surface irregularities, thus ensuring sound adhesion. Again, such mechanical bonding is typical of enamel glazes on materials [30].

7. Conclusion

Contact angle measurements revealed that because of the wettability characteristics of the AOC, laser surface treatment was necessary in order to allow the enamel to wet and adhere to the AOC surface. As such, the laser treatment of the AOC surface resulted in the contact angle decreasing from 118^0 to 33^0. Wetting, and subsequent bonding, of the enamel to the AOC surface after laser treatment was identified as being due to:

1. The laser sintering of the AOC surface reducing the surface roughness from an Ra value of $25.85\mu m$ before laser treatment, to $6.27\mu m$ after laser treatment, thus directly reducing the contact angle θ.

2. The increase in the polar component of the surface energy γ_{sv}^{p}, (2.00 mJm^{-2} to 16.15 mJm^{-2}) after laser treatment as a result of the partial laser vitrification of the glass forming elements within the AOC composition, thus improving the action of wetting and adhesion.

3. The 36.29% increase in the surface oxygen content of the AOC resulting from laser treatment was identified as further promoting the action of wetting.

The bonding mechanisms of the enamel to the AOC were identified as being principally the result of van der Waals forces due to the chemical nature of the AOC. However, evidence of some chemical bonding due to some of the base AOC material dissolving into the enamel glaze was observed.

This work demonstrates that it is possible to alter the wetting characteristics of the AOC using the HPDL to facilitate the firing of a vitreous enamel onto the AOC surface, a task not possible without laser treatment. But, moreover, the findings of this work show that with the use of laser radiation it is a distinct possibility that the wetting characteristics of many other materials could be altered.

Acknowledgements

References

1. M. UEKI, M. NAKA and I. OKAMOTO, *J. Mater. Sci. Lett.* **5** (1986) 1261-1262.

2. P. NIKOPOULOS, and D. SOTIROPOULOU, *J. Mater. Sci. Lett.* **6** (1987) 1429-1430.

3. P.R. CHIDAMBARAM, G.R. EDWARDS and D.L. OLSON, *Mater. Trans. B* **23** (1992) 215-222.

4. J.G. LI, *J. Mater. Sci. Lett.* **11** (1992) 903-905.

5. J.G. LI, *Mater. Lett.* **22** (1995) 169-174.

6. V.W. GUTOWSKI, L. RUSSELL and A. CERRA, in "Science and Technology of Building Seals, Sealants, Glazing and Waterproofing: Adhesion of Silicone Sealants to Organic-Coated Aluminium" edited by J.M. Klosowski (ASTM, Philadelphia, 1992) p. 144-159.

7. X.B. ZHOU and J.T.M. DEHOSSON, *J. de Phys. IV* **3** (1993) 1007-1011.

8. X.B. ZHOU and J.T.M. DEHOSSON, *Acta Metall. Mater.* **42** (1994) 1155-1162.

9. J.G. LI, *Rare Met.* **2** (1993) 84-96.

10. T. BAHNERS, W. KESTING and E. SCHOLLMEYER, *Appl. Surf. Sci.* **69** (1993) 12-15.

11. T. BAHNERS, *Opt. & Quan. Elec.* **27** (1993) 1337-1348.

12. J. LAWRENCE, L. LI and J.T. SPENCER, in Proceedings of ICALEO'96: Laser Materials Processing, Detroit, October 1996, p. 138-148.

13. M.J. JAYCOCK and G.D. PARFITT, in "Chemistry of Interfaces" (John Wiley & Sons, Chichester, 1981) p. 234-247.

14. W.A. ZISMAN, in *"Advances in Chemistry Series 43: Contact Angle, Wettability and Adhesion"* edited by R.F. Gould (American Chemical Society, Washington DC, 1964) p. 1-51.

15. A.W. NEUMANN, *Adv. Colloid Interface Sci.* **4** (1974) 438.

16. F.M. FOWKES, *Ind. Eng. Chem.* **56** (1964) 40-52.

17. E.P. DEGARMO, J.T. BLACK and R.A. KOHSER, in "Materials and Processes in Manufacturing" (Prentice Hall, Upper Saddle River, 1997) p. 379.

18. L. PENNISI, in "Engineered Materials Handbook: Ceramics and Glasses" edited by S.J. Schneider (ASM International, Metals Park, 1991) p. 255-259.

19. L.S. O'BANNON, in "Dictionary of Ceramic Science and Engineering" (Plenum Press, New York, 1984) p. 232.

20. W.M. STEEN, in "Laser Materials Processing" (Springer-Verlag, London, 1991) p. 147.

21. D.W. RICHERSON, in "Modern Ceramic Engineering" (Dekker, New York, 1992), p. 217.

22. T.Z. KATTAMIS, in "Laser in Metallurgy" edited by K. Mukherjee & J. Mazumder (AMIE, New York, 1981) p. 1.

23. S. AGATHOPOULOS and P. NIKOLOPOULOS, *J. of Biomed. Mater. Res.* **29** (1995) 421-429.

24. D.L. BOURELL, H.L. MARCUS, J.W. BARLOW and J.J. BEAMAN, *Int. J. Powder Metall.* **28** (1992) 369-381.

25. M. AGARWALA, D.L. BOURELL, J.J. BEAMAN, H.L. MARCUS, and J.W. BARLOW, *Rapid Prototyping J.* **1** (1995) 26-36.

26. D.K. CHATTORAJ and K.S. BIRDI, in "Adsorption and the Gibbs Surface Excess" (Plenum Press, New York, 1984) p. 95.

27. R.J. GOOD and L.A. GIRIFALCO, *J. Phys. Chem.* **64** (1960) 561-565.

28. V.A. GREENHUT, in "Engineered Materials Handbook: Adhesives and Sealants" edited by H.F. Brinson (ASM International, Metals Park, 1991) p. 298-311.

29. J.A. PASK and A.P. TOMISA, in "Engineered Materials Handbook: Ceramics and Glasses" edited by S.J. Schneider (ASM International, Metals Park, 1991) p. 482-492.

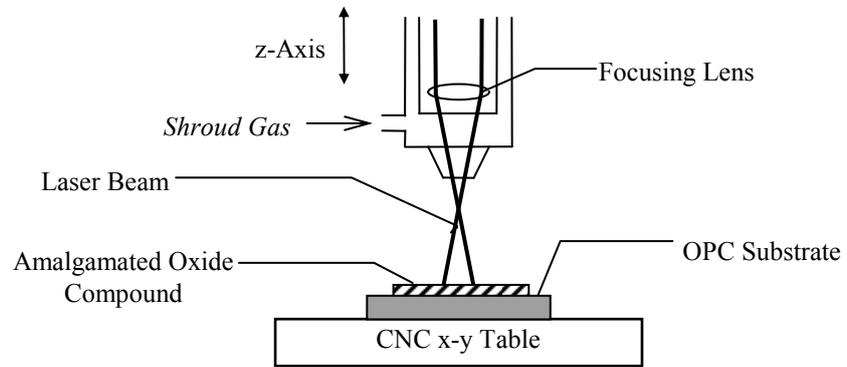30. V.V. VARGIN, in "Technology of Enamels" (MacLaren & Sons, London, 1965) p. 49-56.
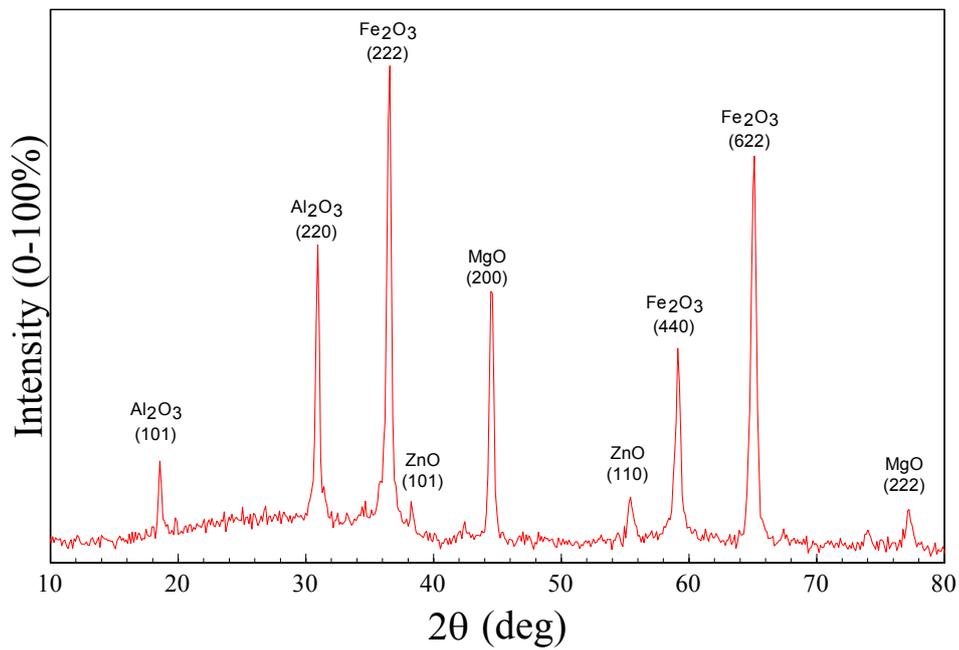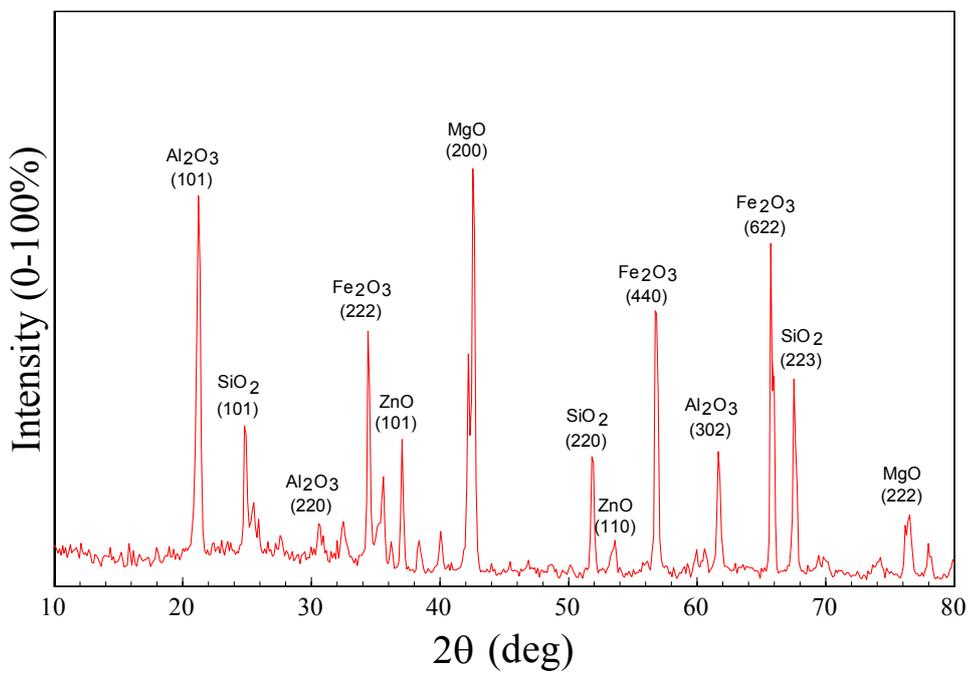
LIST OF FIGURES

Figure 1

Figure 2

(a)
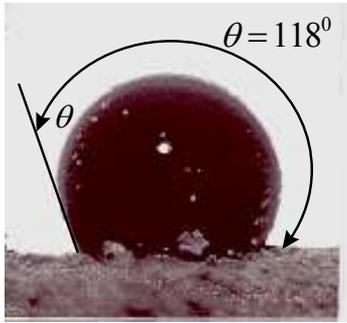
(b)

Figure 3

(b)

(a)

Figure 4

(a)

(b)

Figure 5

$\theta = 118^0$

(a)

$\theta = 33^0$

(b)
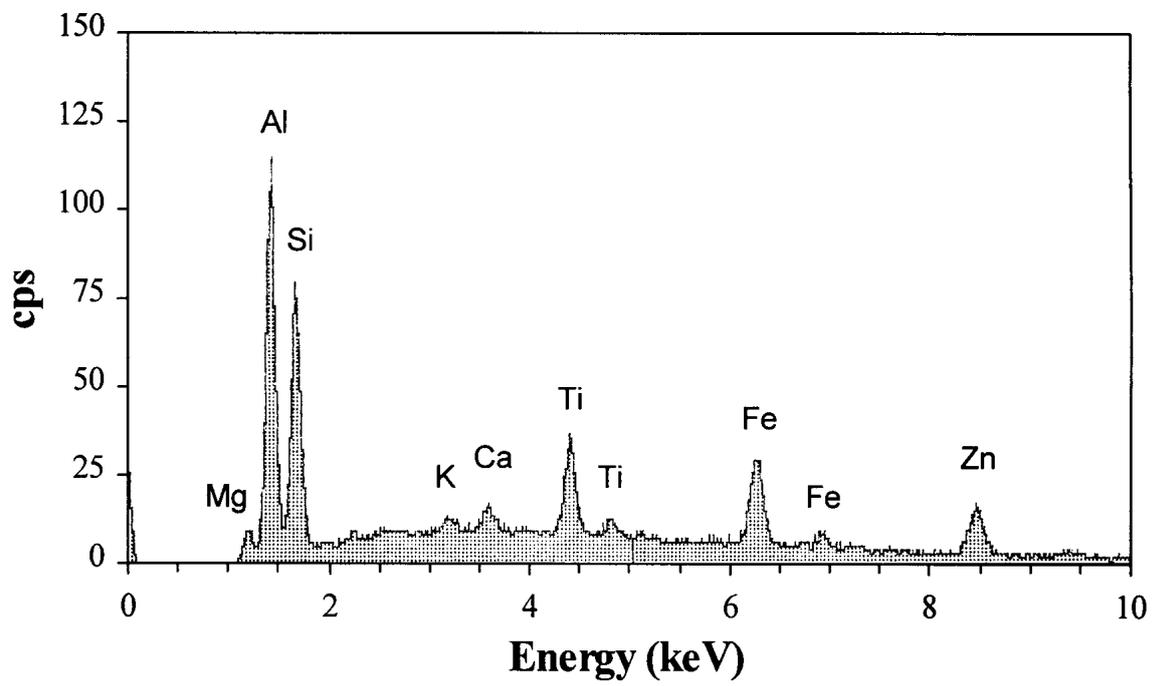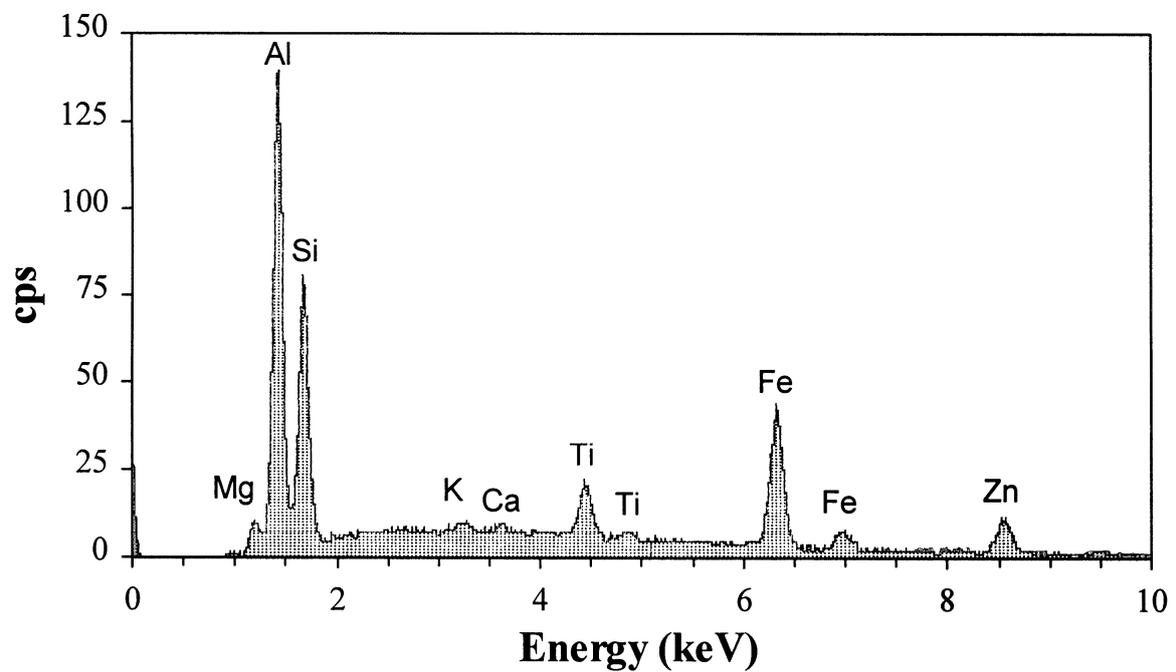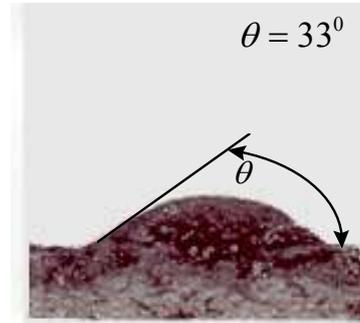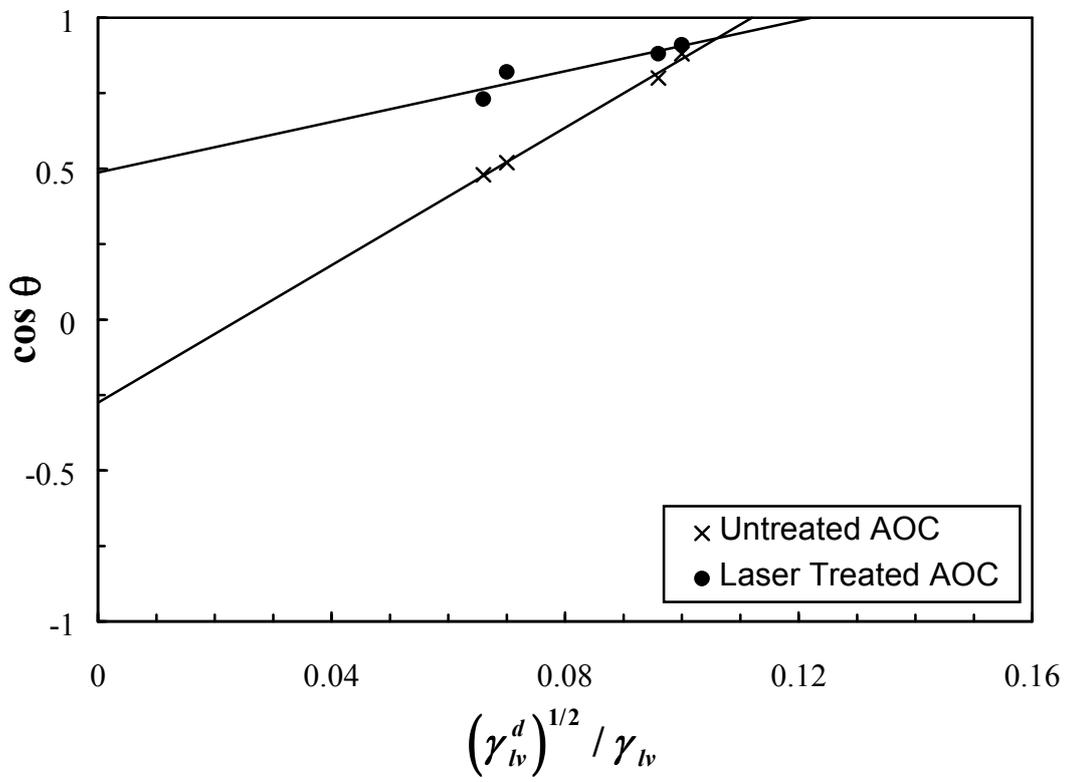
Figure 7

LIST OF TABLES

Table I

Liquid	γ (mJm^{-2})	γ_{lv}^{d} (mJm^{-2})	γ_{lv}^{p} (mJm^{-2})
Human Blood	47.5	11.2	36.3
Human Blood Plasma	50.5	11.0	39.5
Glycerol	63.4	37.0	26.4
4-Octonol	27.5	7.4	20.1

Table II

Surface Energy Component	Untreated AOC	HPDL Treated AOC
Dispersive Component, (γ_{sv}^{d})	84.16 mJm^{-2}	55.69 mJm^{-2}
Polar Component, (γ_{sv}^{p})	2.00 mJm^{-2}	16.15 mJm^{-2}
Total, (γ_{sv})	86.16 mJm^{-2}	71.84mJm^{-2}